HHS Public Access

Author manuscript

Stem Cell Res. Author manuscript; available in PMC 2021 March 04.

Published in final edited form as:

Stem Cell Res. 2020 December ; 49: 102086. doi:10.1016/j.scr.2020.102086.

Distinct molecular profile and restricted stem cell potential defines the prospective human cranial neural crest from embryonic stem cell state

Maneeshi S. Prasad[*], **Rebekah M. Charney**, **Lipsa J. Patel**[1], **Martín I. García-Castro**[*]

School of Medicine Division of Biomedical Sciences, University of California, Riverside, USA

Abstract

Neural crest cells are an embryonic multipotent stem cell population. Recent studies in model organisms have suggested that neural crest cells are specified earlier than previously thought, at blastula stages. However, the molecular dynamics of early neural crest specification, and functional changes from pluripotent precursors to early specified NC, remain to be elucidated. In this report, we utilized a robust human model of cranial neural crest formation to address the distinct molecular character of the earliest stages of neural crest specification and assess the functional differences from its embryonic stem cell precursor. Our human neural crest model reveals a rapid change in the epigenetic state of neural crest and pluripotency genes, accompanied by changes in gene expression upon Wnt-based induction from embryonic stem cells. These changes in gene expression are directly regulated by the transcriptional activity of β-catenin. Furthermore, prospective cranial neural crest cells are characterized by restricted stem cell potential compared to embryonic stem cells. Our results suggest that human neural crest induced by Wnt/β-catenin signaling from human embryonic stem cells rapidly acquire a prospective neural crest cell state defined by a unique molecular signature and endowed with limited potential compared to pluripotent stem cells.

Keywords

Neural crest; Stem cells; Embryonic stem cells; Specification; Neural plate border; Cell fate; Cranial neural crest; Pluripotency

[*]Corresponding authors. maneeshi@ucr.edu (M.S. Prasad), martin.garcia-castro@ucr.edu (M.I. García-Castro).

[1]Current address: Liberty University, Lynchburg, VA, USA.

CRediT authorship contribution statement

Maneeshi S. Prasad: Conceptualization, Methodology, Investigation, Writing - original draft, Writing - review & editing. **Rebekah M. Charney:** Investigation, Writing - review & editing. **Lipsa J. Patel:** Investigation. **Martin I. Garcia-Castro:** Conceptualization, Methodology, Writing - original draft, Writing - review & editing, Funding acquisition, Resources.

Declaration of Competing Interest

The authors declare that they have no known competing financial interests or personal relationships that could have appeared to influence the work reported in this paper.

Appendix A. Supplementary data

Supplementary data to this article can be found online at https://doi.org/10.1016/j.scr.2020.102086.

1. Introduction

Neural crest (NC) is a multipotent embryonic stem cell population that is unique to vertebrates and contributes to a multitude of cell types throughout the developing embryo – including the craniofacial skeleton and peripheral neurons and glia – that generate some of the key features of vertebrate evolution and diversity (Gans and Northcutt, 1983; Glenn Northcutt, 2005; Le Douarin, 1980; Le Douarin and Kalcheim, 1999; Le Douarin and Dupin, 2018). Due to this wide contribution during embryonic development, improper formation of NC leads to numerous neurocristopathies including the highly prevalent cleft lip and cleft palate, rare syndromes such as Hirschsprung's disease, and the pediatric cancer neuroblastoma (Bolande, 1974, 1997, 1996; Etchevers et al., 2006; Farlie et al., 2004). NC cells are fascinating for their unique ability to contribute to terminal derivatives that are known to arise from multiple germ layers. While throughout the body NC contributes to ectodermal derivatives such as peripheral neurons and glia, cranial NC (but not trunk NC) also gives rise "ectomesenchyme" which includes bone, cartilage, and adipocytes. Given these characteristics, the NC has been termed the "fourth germ layer" (Hall, 2018, 2000); however, the molecular mechanisms responsible for this pseudo-mesodermal differentiation capacity remain ill-defined. The specification of cranial NC from a pluripotent cell, rather than from an ectodermally restricted cell, could account for their unique differentiation potential towards both ectoderm and mesoderm derivatives. *In vivo* studies in *Xenopus,* chick, and rabbit have suggested the continued specification of cranial NC during gastrulation (Basch et al., 2006; Betters et al., 2018; Mancilla and Mayor, 1996). Accordingly, this early specification of cranial NC was found to be independent of the definitive mesodermal or neural contributions in chick (Basch et al., 2006). Furthermore, recent work in *Xenopus* (Buitrago-Delgado et al., 2015) and chick (Prasad et al., 2020), has suggested a blastula stage origin of NC, implying the initiation of the NC specification program from pluripotent epiblast cells at blastula stage.

To advance both basic and translational research of human biology and pathology, human pluripotent stem cell (hPSCs) based models have been extensively used to address developmental processes and molecular mechanisms involved in cell fate decisions (Evans, 2011; Funa et al., 2015; Pera and Trounson, 2004; Rodda et al., 2002; Sasai, 2013; Spagnoli and Hemmati-Brivanlou, 2006; Ying et al., 2015). Due to accessibility and ethical limitations, there have only been a few embryological studies on human neural crest (hNC) (Betters et al., 2010; O'Rahilly and Müller, 2007; Wilderman et al., 2018). Recently, our lab and others have harnessed the enormous potential of human pluripotent stem cells to examine human NC biology (Chambers et al., 2016; Fukuta et al., 2014; Gomez et al., 2019a, 2019b; Hackland et al., 2017, 2019; Huang et al., 2016; Lee et al., 2010; Leung et al., 2016; Menendez et al., 2011; Mica et al., 2013; Umeda et al., 2015). Our lab has developed a rapid and robust model of human NC formation which provides unlimited, synchronized cranial NC cells based on WNT activation alone (Gomez et al., 2019a; Leung et al., 2016) (Fig. 1A). Importantly, our hNC model (Leung et al., 2016) is in alignment with studies in embryonic model organisms regarding the critical role of WNT/β-catenin signaling with additional requirement of FGF and BMP signaling in NC induction (Garcia-Castro et al., 2002; Ikeya et al., 1997; Ko et al., 2007; LaBonne and Bronner-Fraser, 1998; Oka et al.,

2009; Saint-Jeannet et al., 1997; Stuhlmiller and Garcia-Castro, 2012a,b). While NC models from other groups (Chambers et al., 2016; Menendez et al., 2011; Mica et al., 2013) have used TGFβ inhibition for generating NC, our hNC model is significantly different, as we have demonstrated the necessity of intrinsic TGFβ as well as BMP and FGF signaling in NC formation (Leung et al., 2016) in agreement with the embryological evidence (Ko et al., 2007; Oka et al., 2009). Furthermore, in alignment with studies of early NC ontogeny in chick (Basch et al., 2006; Prasad et al., 2020), in our hNC model, formation of human cranial NC is independent of mesodermal or neural contributions (Leung et al., 2016). Our previous studies (Gomez et al., 2019b, 2019a; Leung et al., 2016) have thus elaborated on signaling requirements during human NC formation in our hNC model; however, much remains to be understood about the molecular and functional events leading up to the formation of cranial NC cells from the pluripotent stem cell (PSC) state.

In this study, we took advantage of our improved hNC model (Gomez et al., 2019a) (Fig. 1A) to interrogate the molecular and functional events associated with early human cranial NC formation from pluripotent human embryonic stem cells (hES). We report rapid and distinct changes in the epigenetic and transcriptional state of human prospective neural crest (pNC) cells from hES at a high temporal resolution, suggesting critical changes in cell fate potential. In agreement with the crucial role of Wnt/β-catenin pathway in NC formation (Garcia-Castro et al., 2002; Ikeya et al., 1997; LaBonne and Bronner-Fraser, 1998; Leung et al., 2016; Saint-Jeannet et al., 1997), β-catenin transcriptional activity along with its target gene, GBX2, were found to be necessary for the initiation of the gene expression program required for human NC formation. Crucially, functional analysis testing the stem cell potential of early NC cells (pNC) revealed a clear restriction in potential of pNC to form mesoderm and endoderm, exposing key differences between pNC and pluripotent ES cells. Our results suggest that the cranial human NC arise from the pluripotent stem cells, progressing through a prospective NC state characterized by a distinct molecular signature and a limited differentiation potential compared to ES cells, which is in alignment with the multipotent character of NC. This study provides insights into the molecular and functional differences at the earliest stages of human cranial NC specification from the ES cell state.

2. Methods

2.1. hESC growth and maintenance

H1 human embryonic stem cells (WA01, WiCell Institute) of passages 24 to 35 were maintained on plastic surfaces coated with Matrigel (08-774-552, Fisher Scientific) in serum-free medium (mTeSR1, STEMCELL Technologies). Cultures were passaged every 4 to 5 days using Versene (Lonza) according to the manufacturer's instructions. Cells were routinely tested for mycoplasma contamination using Lonza Bio-science's MycoAlert detection kit. Current reading for H1 hES cells p29 was 0.71738, well within the <0.9: Negative for mycoplasma range for the test. Cell line has been validated using STR analysis as per WiCell certificate of analysis.

2.2. Neural crest, non-neural ectoderm, neural ectoderm, mesoderm and endoderm differentiation

For neural crest induction, human ESC/iPSC colonies were treated with Accutase cell detachment solution (STEMCELL Technologies) and re-suspended in induction medium plus 3 μM CHIR 99021 and 10 μM ROCK inhibitor, Y-27632 (Tocris Bioscience) plated at the 20,000 cells/cm2 density on Matrigel-coated surfaces. Induction medium contained DMEM/F12 medium supplemented with 2% B27 supplement (Gibco), 1X Glutamax (Gibco) and 0.5% bovine serum albumin (wt/vol) (Sigma-Aldrich). CHIR and ROCK inhibitor Y-27632 were added for the first two days, induction media without CHIR and ROCK inhibitor was used for next 3-days. For non-neural ectodermal differentiation, basal media with 2% B27, 1x Glutamax, and 0.5% BSA was used for 5 days (Leung et al., 2016). For neuroectodermal differentiation, DMEM/F12 medium with 2% B27 supplement, 1 × Glutamax, 100 nM LDN-193189 (Tocris) and 10 μM SB431542 (Tocris) was used for 5 days (Leung et al., 2019). For mesoderm induction, DMEM/F12 supplemented with 2.5 ng/ml FGF basic (Tocris Bioscience) with 3 μM CHIR was used for 3 days, while for endoderm induction DMEM/F12 supplemented with 1% FBS and 10 ng/ml Activin A (Tocris Bioscience) with 3 μM CHIR was used for first day and without CHIR next two days. Plating density for all differentiation were maintained at 20,000 cells/cm2. Small molecules and medium were replenished daily.

2.3. Wnt/β-catenin signaling modulation

For XAV939 (Cayman Chemicals # 13596) mediated inhibition of Wnt/β-catenin signaling, the hES cells were processed for NC induction as described above and 5 μM XAV939 and 3 μM CHIR 99021 was added to the NC induction media prior to plating the cells on day 0.5 μM XAV939 and 3 μM CHIR 99021 was maintained in the media for day 1 media change. For Wnt3a mediated NC induction, exactly the same protocol was followed as for CHIR 99021, but instead of CHIR 99021, 10 ng/ml of Wnt3a was used. Cell were harvested at day 5 by 10 min fixing in 4% paraformaldehyde for immunofluorescence.

2.4. siRNA mediated knockdown

siRNA mediated knockdown was performed using Silencer Select siRNA for CTNNB1 (β-catenin) (Thermo Scientific cat.# AM51331), GBX2 (Thermo Scientific cat.# 4427037) and non-targeting control (NTC) siRNA (Thermo Scientific cat.# AM4621) transfected with Lipofectamine RNAiMAX (Thermo Scientific cat. # 13778075). Reverse transfection was performed as per manufacturer's instructions. Briefly, siRNA/RNAiMAX mixture was pre-plated into the 96 well plate in technical replicate for each biological replicate. Human ES cells were plated in NC induction media as described above into each of the wells containing siRNA/RNAiMAX mixture. For each well 1.2 picomole of siRNA was used with 0.1 μl of Lipofectamine RNAiMAX reagent in total 20 μl of OptiMEM medium. Media was changed every 24 h and cells were harvested at day 2, 3 and 5 for RNA extraction and day 5 for immunofluorescence.

2.5. Terminal differentiation of neural crest cells

NCCs at day 5 and hES cells at 70–80% confluency were treated with accutase and plated at 20,000–100,000 cells/cm2 on a Matrigel or PO/ Laminin/Fibronectin coated surface in respective differentiation medium, supplemented with 10 μM Y-27632. Medium was changed 24hrs after plating to terminal differentiation media without Y-27632. All differentiation experiments were performed at least in 4 separate biological replicates. Differentiation protocols used are described in Leung et al. (2016) and adapted from Studer lab group, except chondrocyte differentiation (Chambers et al., 2012; Lee et al., 2007b; Mica et al., 2013). Briefly, **Osteogenic differentiation**: Neural crest cells are plated at 300,000 cells/cm2 in osteogenic differentiation media (10 mM β-glycerol phosphate, 0.1 μM dexamethasone and 200 μM AA in α-MEM medium containing 10% FBS) and media is changed every 2–3 days for 21 days when calcification can be seen. Cells were stained with alizarin red for calcification. **Chondrogenic differentiation**: Mesencult-Chondrogenic Differentiation media (Stem cell technologies) was used as per the supplier's protocol. Chondrocyte pellets at the end of the protocol were paraffin sectioned and stained with Alcian blue. **Adipogenic differentiation**: Neural crest cells at day 5 were dissociated with accutase and plated at 50 K/cm2 density in adipogenic media (1 mM dexamethasone, 10 μg/ml Insulin and 0.5 mM IBMX in α-MEM medium containing 10% FBS) with media changes every 2–4 days for 21 days and then stained with oil red. **Myofibroblast differentiation**: Neural crest cells at day 5 were dissociated and plated at 50 K/cm2 density in alpha-MEM with 10%FBS for 14 days. Cells were stained with smooth muscle actin (Sigma, A2547 at 1:500) and S100β (abcam, ab52642 at 1:200). **Peripheral neurons differentiation:** On day 5 of NC induction, nociceptor induction was initiated with the addition of perineural media (3 μM CHIR99021, 10 μM SU5402 and 10 μM DAPT, in N2/ DMEM/F12). Cells were harvested after 5 days to test for Peripherin (Millipore AB1530 at 1:200) and HuC/D (Molecular Probes, A-21271 at 1:300). **Glial cell differentiation**: NC cells on day 5 were plated on to PO/Laminin/Fibronectin coated wells in DMEM/F12/N2 medium supplemented with 10 ng/ml of FGF2 and 10 ng/ml of EGF for 14 days. After FGF2/EGF culture, cells are differentiated towards Schwann cell lineage in N2 medium supplemented with ciliary neurotrophic factor (10 ng/ml), neuregulin (20 ng/ml), FGF2 (10 ng/ml) and cyclic AMP (0.5 mM) for 21 days. Cells were stained with S100β. **Melanocyte differentiation**: On day5 of NC induction, melanocyte differentiation media was added (25 ng/ml BMP4 and 100 nM EDN3 in DMEM/F12/N2) for 5 days. Cells were further passed on to PO/Lamini/Fibronectin coated wells in Mel Maturation media (Neurobasal/Mel Media as described in Mica et al., 2013) for another 2–3 passage then stained for Sox10/MITF (R&D systems, AF5769 at 1:100).

2.6. Gene expression analysis

For human ES/NC cells: Total RNA was extracted using TRIzol reagent/DirectZol kit (Zymoresearch). Total RNA (0.5–1 μg) was reverse-transcribed using PrimeScript reverse transcriptase kit (Takara/Clontech Laboratories). Quantitative polymerase chain reaction (QPCR) was carried out using the SYBR Premix ExTaqII SYBR Green premix (Takara/ Clontech Laboratories) on Applied Biosystems QuantStudio 6 Real-Time PCR System (Applied Biosystems). Primer concentration of 300 nM was used. Primer sequences are

listed in Supplemental Table 1. For statistical analysis, three to five biological replicates were measured for each experiment using ΔΔCT method relative to ES cell state and normalized to GAPDH. Four reference keeping genes (GAPDH, HPRT1, 18 s, RPL13) were analyzed and gene (GAPDH) with lowest standard deviation (<0.3) over the time course of NC induction was used.

2.7. Chromatin immunoprecipitation

ChIP assays were carried out with modified version of ChIP protocol previously described (Tsankov et al., 2015). Briefly, cells were cross-linked with 1% formaldehyde, quenched in 0.125 M Glycine and flash frozen. Following lysis in RIPA buffer, chromatin was sonicated to a fragment size of 300–400 bp using Covaris S220 Focused-ultrasonicator (Covaris). Solubilized chromatin was immunoprecipitated with H3K27me3 (Active Motif, 39155), H3K4me3 (Active Motif, 39159) and H3K27ac (Abcam, ab4729). Immunoprecipitated DNA was eluted and analyzed for enrichment using ChIP-QPCR. Data is represented from 3 biological replicates as percent input values. Primer sequences are listed in Supplemental Table 1.

2.8. Immunofluorescence for hES/hNC cells

Immunofluorescence was performed on cells cultured on Nunc Lab-Tek Permanox Chamber Slide System (Thermo Scientific, #177410), 24-well plate and 48-well plate as previously described (Leung et al., 2016). Primary antibodies are listed in Supplemental Table 1. Secondary antibodies were species- or subtype-specific Alexa secondary antibodies (Thermo Scientific). Images were taken using a Nikon Eclipse Ti microscope or Zeiss Confocal (Zeiss 880 Inverted microscope) and analyzed using Nikon Elements software (Nikon). Images were processed in Adobe Photoshop and were simultaneously adjusted.

2.9. Image processing and cell count analysis for hES and hNC cells

Images in Fig. 3 (except for ZIC3 image) were taken on Zeiss Confocal (Zeiss 880 Inverted microscope) at the UCR Microscopy and Imaging Core Facility and images in Figs. 5 and 6 were taken on Nikon Eclipse Ti inverted microscope at UCR Stem Cell Core Facility. All images were taken at the same exposure (PMT/laser) setting for each antibody over the time course. Image exposure settings were set using the time point with highest expression of the particular protein. Images were further assembled in Photoshop and edited simultaneously for exposure levels and sharpness. Nikon Elements software (with General Analysis) (Nikon) was used for cell count analysis. For cell count analysis, under general analysis, bright spot detection method was used, with clustered object parameter, with variable object (cell) sizes depending on the sample, determined manually for each sample to detect every cell in the image under each channel. No primary control was used to subtract the background fluorescence for all the samples in an experiment equally. Unmodified images were used to obtain total cell counts and plotted as bar graphs from each individual experiment. Each experiment was done in 3–4 biological replicates.

2.10. Western blotting and quantification

Cells were lysed using RIPA lysis buffer (50 mM Tris-HCl pH 7.4, 150 mM NaCl, 5 mM EDTA, 0.5% sodium deoxycholate, 1% NP40, 0.1% SDS), supplemented with protease inhibitors (Roche Diagnostics), followed by centrifugation to remove cell debris, supernatant was collected as the total protein lysate. Protein quantification was performed using the Bradford Protein Assay (Bio-Rad). 30μg of total protein samples in Lammeli buffer with β-mercaptoethanol were separated on a 10% SDS-PAGE gel and transferred to nitrocellulose membrane (BioRad). Membrane was blocked with 5% milk and incubated with the primary antibodies, anti-Pax7 and anti-Pax3 (1:500, Developmental Studies Hybridoma Bank), ZIC3 (Sigma, HPA069523, 1:500), Oct4 (SCBT, sc-5279, 1:500), SOX2 (SCBT, sc-365823, 1:500), anti-β-actin (A5316, Sigma-Aldrich; 1:10,000) or GAPDH (AM4300, Thermo Fisher Scientific, 1:10,000) for 1hr at room temperature. Membrane was then incubated with a horseradish peroxidase-conjugated secondary antibody, goat anti-mouse IgG (H + L) (Thermo Fisher Scientific, 31432). Signal was developed using the Clarity Western ECL Kit (BioRad) and detected using x-ray films or Chemidoc Gel imaging system (BioRad). Western blot bands were quantified using Image J densitometry, normalized to background and further to the reference gene β-actin or GAPDH to obtain normalized intensity values. Westerns were done for 3–4 separate biological replicates.

2.11. Statistical analysis

For ChIP-qCPR, RT-qPCR and other quantitative measurements throughout the manuscript, graphs were created, and statistical analyses were performed using the GraphPad software Prism (version 7). Asterisks indicate statistical significance: *P ≤ 0.05, **P ≤ 0.01, ***P ≤ 0.001, ****P ≤ 0.0001. Unpaired t-tests and one-way ANOVA tests were respectively performed for comparisons of two or more means. Graphs represented throughout the manuscript are derived from 3 or more experiments. Heatmap in supplement Fig. 1 Fig. S1A was generated using Pheatmap.r R-package using R-program (R-Studio). Briefly, data from RT-qPCR analysis used to generate the heatmap in Fig. 2A, was used in Pheatmap.r package for unbiased clustering of the gene expression data.

3. Results

3.1. Human prospective neural crest cell state is defined by distinct epigenetic changes

Early events in embryonic development have a significant effect on the health of the fetus, including the specification and formation of NC. Studies in model organisms have revealed that specification of NC is ongoing at gastrula stage (Basch et al., 2006; Betters et al., 2018; Mancilla and Mayor, 1996; Patthey et al., 2008), while a recent study from our group points to a population of prospective NC (pNC) cells that are specified from the pluripotent chick blastula epiblast (Prasad et al., 2020). However, the molecular mechanisms underlying the early NC specification and relationship between pluripotent cells and NC cells is unknown. To assess the molecular character of pNC, we made use of our hNC induction protocol based on exogenous activation of Wnt/β-catenin signaling for two days using a small molecule inhibitor of GSK3 (CHIR99021) which triggers the stabilization of β-catenin and promotes the formation of NC from hES cells (Gomez et al., 2019a) (Fig. 1A). We first interrogated temporally the epigenetic status of proximal promoter regions of pluripotency and NC genes

using the ChIP-qPCR assay. Changes in epigenetic state has provided a very early marker for distinguishing cell fate choices during cell fate specification from pluripotent stem cells (Lee et al., 2007a; Voigtet al., 2013b;Petruk et al., 2017; Spivakov and Fisher, 2007). Analysis of changes in histone modifications of pluripotency and differentiation genes is a crucial avenue of exploration to study lineage specification. To address the change in cell state from pluripotent stem cell state at the epigenetic level, we analyzed key histone modification marks, H3K27ac, H3K4me3 and H3K27me3 (representative of active or repressed gene states), during the 5 days of NC induction.

We analyzed cells during the first 24 h of NC formation from hES to address the earliest time point during NC differentiation, and also included cells at Day 3 (neural plate border) and at Day 5 (NC) of NC induction. We utilized the proximal promoter regions of ES and NC genes identified from previously published ChIP-Seq datasets of later stage hNC (derived from hES cells) (Rada-Iglesias et al., 2012, 2011). Compared to ES cell state we saw clear differences in the enrichment of activation (H3K27ac, H3K4me3) and repression (H3K27me3) marks at the proximal promoter region of stem genes (OCT4, NANOG, KLF4) and NC genes (PAX3, PAX7, ZIC3). The proximal promoters of stemness genes OCT4, NANOG, KLF4, displayed an immediate loss of the activation marks H3K27ac/H3K4me3, and a gain of the polycomb repression mark H3K27me3 within the first 6 h (Fig. 1B). The proximal promoter of NC genes PAX3, PAX7, and ZIC3, on the contrary, showed enrichment of the H3K27ac/H3K4me3 marks with a loss of H3K27me3 within the first 6 h (Fig. 1B). At day 3 and day 5, a progressive gain in the activation mark with loss of repressive mark was further seen at proximal promoter of NC genes, including Sox10 at this stage, and vice versa for stem gene promoters (Fig. 1C). These findings indicate a rapid change in cell fate decision from an ES cell state to a pNC cell state, and underscore the molecular differences underlying these cell fates.

3.2. Distinct dynamic gene expression changes define the pNC cell state

3.2.1. Unique molecular signature of the pNC cell state—We next asked whether the changes in epigenetic status of pluripotency and NC gene promoters are associated with transcriptional changes reflecting a NC character. Therefore, we assayed for gene expression profiles at high temporal resolution for 7 stem cell genes and 18 genes known to comprise the core NC gene regulatory network (Prasad et al., 2019, 2012; Sauka-Spengler and Bronner-Fraser, 2008; Simoes-Costa and Bronner, 2015). To address the immediate changes following NC induction from hES cells, gene expression was assayed at 6 h intervals within the first 24 h of hNC induction and every 24 h thereafter through day 5. RT-qPCR analyses revealed dynamic changes in gene expression in the transition between ES to a NC cell state. Based on known expression patterns of these NC-related genes in model organisms, we grouped our model of hNC induction into 3 phases: NC Phase-I (NC-I, 6 h-day 2) consisting of prospective NC cells that defines a pre-Border state, NC Phase-II (NC-II, day 2–4) consisting of pNC cells that contribute towards neural plate border (NPB) state and NC Phase-III (NC-III, day 4–5) consisting of proper NC cells (Fig. 2A). An unbiased hierarchical clustering of this data also eludes to groups of genes that are dynamically changing during NC specification, and supports the notion that the hierarchy of NC factors

identified in model organisms is generally conserved during human cranial NC formation (Fig. S1A).

Within each phase, we observed striking dynamics between NC factors and stemness genes. At 6 h post induction, pNC displays significant activation of a subgroup of NC genes (i.e. PAX3, PAX7, MYB, ZIC3, GBX2), which we now refer to as the earliest genes associated with pNC cells in NC-I or pre-Border state (Fig. 2A and B). Similar early changes in NC gene expression were also observed by another study during the first 24 h of Wnt-activation (Funa et al., 2015). By day 2, we observed an initial expression of NC-II genes SOX5 and SOX9. At day 3, pNC cells display stronger levels of NC-I genes (except MYB) and now activate a cohort of NC-II genes including ID2, MSX1, MSX2, SNAI2, SOX5, and SOX9 (Fig. 2A and Fig. S1B). Finally, at day 5, NC cells exhibit expression of NC-III genes FOXD3, SOX10 and ETS1, in addition to the retention of many NC-I and NC-II genes, with the exception of GBX2 and ZIC3 (Fig. 2A and Fig. S1B). At the same time, we examined the temporal dynamics of stem marker expression. Compared to the ES cell state, at 6 h we observed an upregulation of SOX2 and KLF4, and a downregulation of FOXD3, MYC and TFCP2L1, suggesting an unbalanced stem cell state and clear departure from an ES cell state (Fig. 2B). By 24 h, pNC show unchanged OCT4 levels, an upregulation of SOX2 and KLF4, and a significant reduction of NANOG, TFCP2L1, and MYC – further suggesting a departure from an ES cell state (Fig. 2B). At 48 h there is further reduction in the expression of OCT4 and other core stemness genes, with the exception of SOX2 which continues to increase (Fig. 2B and Fig. S1B). By day 3 onwards, we observed a sharp decrease in expression of stemness genes, which continues through until day 5 (Fig. S1B). These data reveal a rapid activation of the NC gene program directly from an ES cell state, with drastic changes in the expression of the stemness genes.

We further assessed the expression levels of ectodermal, mesodermal and endodermal genes during early to late stages of NC differentiation in our human NC model. The level of expression of ectodermal genes in NC cells compared to their expression during ectodermal specification has not been assessed due to heterogeneity of these cell populations in the developing embryo. Previously, we demonstrated that there is no significant expression of non-neural ectodermal genes in our NC differentiation culture (Leung et al., 2016). Here we further analyze the temporal expression of non-neural ectodermal (NNE) genes, along with neural ectodermal (NE), mesodermal (Meso), and endodermal (Endo) genes during NC formation. Simultaneously, each of these cell fates (NNE, NE, NC, Meso, Endo) were differentiated from ES cells under cell fate specific defined culture conditions in 3 biological replicates. Cells in precursor and differentiated states were collected at daily time points for each cell fate and analyzed for cell fate specific markers. We observed very low or no expression of NNE, NE, Meso, and Endo genes at any time point (day 1 to day 5) during NC differentiation when compared to the same time points during differentiation of the respective cell fates (Fig. 2C). The very low level of expression of ectodermal genes in NC cultures strongly suggest the absence of ectodermal cells. However, early ectodermal genes may still play a shared role during early stages of NC formation that has not yet been characterized.

3.2.2. Distinct stoichiometric changes in pluripotency factors characterizes pNC cell state—Our gene expression analysis provides robust evidence of dynamic transcriptional changes during NC development, and in particular during the first 24 h of hNC induction. To assess if transcriptional changes were accompanied by changes in levels of protein expression during the ES to pNC fate transition, we performed high resolution temporal analysis of protein expression. We analyzed the protein levels of OCT4, NANOG, SOX2, PAX3, PAX7, and ZIC3 every 6 h during the first 24 h of NC induction from hESCs using immunofluorescence and western blot analysis in biological triplicate (Fig. 3A and B). Immunofluorescence images were taken as 9 frames per well for each gene, performed in technical replicates and repeated over 4 independent biological replicates, in total contributing to 72 single frame images for each gene from 4 biological replicates. Representative images are presented as a single frame in Fig. 3 and Fig. S2. OCT4 and NANOG protein levels decreased within the first 24 h and dropped significantly after day 2 (Fig. 3A). Importantly, we observed a greater than 50% reduction in OCT4 protein levels within the first 24 h, known to be an indicator for the loss of pluripotency (Niwa et al., 2000) (Fig. 3A). SOX2 expression increased within the first 24 h (Fig. 3A), reducing down to ES cell levels by day 5 (Fig. S2). Quantitative western blot analyses confirmed these expression changes (Fig. 3B), suggesting a clear and rapid change in the stoichiometric levels of the stem genes at the onset of NC induction. While we observe a maintenance of OCT4 transcript in pNC (Fig. 2B) that has also been suggested in *Xenopus* (Buitrago-Delgado et al., 2015), we report significant changes in OCT4 protein levels during the first 24hr in pNC, suggesting a change in pluripotency of pNC. The expression of NC genes PAX3, PAX7 and ZIC3 was detected at 6 h and increased progressively within the first 24 h (Fig. 3A). This is the first report of PAX3 and PAX7 protein expression at such an early time point. The level of expression of both these NC factors was significantly lower within the first 24 h compared to significantly higher expression at day 3 and later, as assessed using immunostaining (Fig. 3A and Fig. S2). To identify these low expression levels, rigorous controls were used (e.g. no primary antibody control, single antibody staining at each time point). Exposure levels for each protein staining was set based on day 1 NC sample and used throughout the 24hr time course for comparison. To assay the daily expression levels, we used day 5 NC samples as a positive control to set the exposure levels for NC genes. Interestingly, PAX3 expression was observed in the cytoplasm as well as the nucleus during the first 48hrs, with signal restricted to the nucleus by day 3 (Fig. 3 and Fig. S2). Similar patterns of PAX3 expression have been previously observed (Doddrell et al., 2012). Regardless of the lower expression levels, we further confirmed statistically significant expression of PAX3, PAX7 and ZIC3 within the first 24 h of NC induction from ES cell state using quantitative western blot analysis (Fig. 3B). While ZIC3 is expressed in ES cells, its expression was increased in pNC cells from day 1 (Fig. S2). In addition to the early expression of ZIC3, PAX7, and PAX3, expression of other known NC genes was also analyzed (Fig. S3). Expression of SOX9 protein was detected at day 3, while migratory NC makers p75 and SOX10 were robustly expressed at day 5 of NC differentiation (Fig. S3). Taken together, the epigenetic, transcriptional, and protein expression data presented here demonstrate significant molecular changes in gene expression within the first 6 h of NC induction, with definite stoichiometric changes in stemness gene expression at the RNA and protein levels, suggesting a change in stem cell potential away from the pluripotent state.

3.3. Transcriptional activity of β-catenin is necessary for specification of NC cell fate

Our human NC model relies on the activation of Wnt/β-catenin signaling for the minimal time (first two days) necessary to initiate the NC cell fate (Gomez et al., 2019a). This temporal activation is based on the well documented requirement of Wnt/β-catenin signaling in NC specification in vertebrate model systems (Garcia-Castro et al., 2002; Ikeya et al., 1997; LaBonne and Bronner-Fraser, 1998; Leung et al., 2016; Saint-Jeannet et al., 1997; Huang et al., 2016; Menendez et al., 2011), and is accomplished through activation of Wnt/β-catenin signaling using small molecule CHIR which inhibits GSK3β mediated degradation of β-catenin. However, the temporal role of β-catenin during early human NC specification using Wnt-only activation has not been assessed. To validate that early specification of NC is mediated through the activation of Wnt/β-catenin signaling by CHIR in our newly modified 2 day CHIR protocol, we utilized an inhibitor of Wnt/β-catenin signaling at the intracellular level, XAV939 (a WNT inhibitor that stabilizes Axin, a key component of the β-catenin destruction complex; (Huang et al., 2009)). Using CHIR-mediated NC induction, the cells were treated for the first two days with XAV939 (Fig. 4A). We found that treatment with XAV939 resulted in the inhibition of NC formation as seen by loss of SOX10/PAX7 expression (Fig. 4B) at day 5. This suggests an early direct role of β-catenin in NC formation. Our human NC specification data is further supported by our recent report on the early role of β-catenin in the specification of NC cells at blastula stage of chick embryonic development (Prasad et al., 2020). To further assess the Wnt/β-catenin signaling mediated NC induction, Wnt3a ligand was used to activate Wnt/β-catenin signaling for 2 days (Fig. 4A). As expected, Wnt3a induced robust expression of NC markers, SOX10/PAX7 at day 5 (Fig. 4C), similar to the CHIR-based NC induction (Fig. 4B). Similarly, XAV939 effectively inhibited Wnt3a-mediated NC formation (Fig. 4C). These results clearly suggest that a β-catenin-mediated transcriptional response is necessary for NC formation, corroborating previous results from our group using a model of NC formation with a longer WNT exposure (5 day CHIR protocol) (Leung et al., 2016).

To address the underlying regulatory mechanism resulting in the drastic changes in gene expression (Fig. 2A), we decided to assess the transcriptional targets of β-catenin in human NC formation. We first analyzed the expression of known Wnt/β-catenin target genes, AXIN2 and LEF1, over the 5-day time course of NC induction. The expression of AXIN2 and LEF1 increases progressively from 6 h to day 5 (Fig. 4D). Thus, we assessed the β-catenin-mediated gene expression changes by directly inhibiting β-catenin expression using a siRNA-mediated CTNNB1 (β-catenin) knockdown (Fig. 4E). Knockdown of β-catenin led to the complete loss of SOX10/PAX7 expression (Fig. 4F), validating its crucial role in NC formation. To assess the temporal downstream targets through which the β-catenin response is mediated, we assayed for changes in expression of the key genes identified to be highly expressed during different phases of NC formation (Fig. 2A). Expression of genes from pNC, NPB, NC clusters (Fig. 2A) as well β-catenin (CTNNB1) itself (Fig. 4G: Day2 graph) were all downregulated upon knockdown of β-catenin (Fig. 4G), suggesting an upstream role of β-catenin in regulating the expression of these genes. To validate the β-catenin-mediated regulatory network, we analyzed the effect of knocking down one of the known Wnt/β-catenin target genes during early NC formation, GBX2 (Li et al., 2009). GBX2 is highly expressed during the first 72 h of NC induction (starting at 6hr and up to the NPB

phase), and progressively decreases by day 5 (Fig. 2B). Hence, we initiated siRNA-mediated knockdown of GBX2 at the time of plating (time zero). GBX2 knockdown inhibited the expression of NPB genes (MSX1/2, PAX3/7, SOX5) at day 3, and NC genes (ETS1, FOXD3, SOX9/10, TFAP2) at day 5 (Fig. 4H), as well as its own expression (control) (Fig. 4H: Day2 graph). However, loss of GBX2 did not affect most of the pNC genes, as only GBX2, ZIC1, and TFAP2 were affected (Fig. 4H). The results from this analysis are in agreement with previous findings from Wnt regulation of PAX3 (Bang et al., 1999) and GBX2 perturbation analysis in *Xenopus* (Li et al., 2009), demonstrating the regulation of key NC genes MSX1, PAX3, and FOXD3. The results presented here suggest that GBX2 functions downstream of WNT/β-catenin to active the NPB state during hNC formation.

3.4. Prospective neural crest has restricted stem cell potential compared to ES cells

The analysis of gene expression changes in NC and pluripotency genes as well as the role of β-catenin-regulated transcription factors provides a strong support for a transient pNC cell state. To assess if these molecular profiles observed during the transition from hESC to prospective hNC are associated with functional changes, we addressed the differentiation capacity of prospective and proper NC compared to ES cells. To validate the multipotent stem cell potential of cranial NC cells (Le Douarin and Kalcheim, 1999; Le Douarin and Dupin, 2018) in our human NC model, hNC cells (day 5 NC SOX10+/PAX7 + cells) and ES cells (as an inherent negative control) were subjected to terminal differentiation assays. We have previously reported robust methods for NC terminal differentiation (Leung et al., 2016; Gomez et al., 2019a). NC and ES cells were independently cultured under identical terminal differentiation conditions to generate osteoblasts, chondrocytes, adipocytes, smooth muscle, peripheral neurons, glia, and melanoblast. Starting with same number of cells from ES and NC, terminal differentiation for each of the 7 NC derivatives was performed separately in 4 biological replicates. As expected, hNC cells generated all these derivatives with high efficiency. For all cell fates terminally differentiated from NC we observed 80%−98% of cells with positive staining for specific cell fate markers (Fig. S4). Quantification of differentiated cell types were performed by scoring cells expressing the specific cell fate marker out of the total DAPI positive cells in the culture at the end of the terminal differentiation. Images for scoring were taken from 4 biological replicates, each with 9–25 frames per well, from each differentiated derivative. In cells differentiated from NC, smooth muscle cells (SMA: 98.31%), peripheral neurons (Peripherin: 98.58%; HuD: 20.46%), Glia (S100β: 96.62%), melanoblast (MITF: 85.04%; SOX10: 85.97%), robust osteoblast (Alizarin red staining), chondrocytes (Alcian blue staining) and adipocyte (Oil red staining) differentiation was observed (Fig. S4). However, ES cells under the exact same terminal differentiation conditions displayed limited or no capacity to differentiate into these cell fates, as they need to go through the transient NC phase to form these derivatives (Fig. S4). These results, perhaps unsurprisingly, expose a clear difference between pluripotent ES and multipotent NC cells.

To address the functional state of pNC during specification, we asked if and when would pNC differ from the pluripotent stem cells? To specifically determine how soon do pNC cells differ in their potential from PSCs, we compared the capacity of pNC cells with ES cells to differentiate into mesoderm or endoderm cells. We first characterized a range of

conditions to induce mesoderm (assessed by expression of TBXT and TBX6), and endoderm (assessed by expression of SOX17 and EOMES) from ES cells using varying doses of FGF and Activin, respectively (D'Amour et al., 2005; Leung et al., 2016) (Fig. S5). We then selected the optimal condition with the lowest inductive signal under which robust mesoderm and endoderm formation is readily obtained from ES cells as assessed by expression of TBXT (mesoderm) and SOX17 (endoderm) (Fig. S5). These conditions were subsequently used to compare the mesoderm and endoderm forming potential of ES and pNC cells from 6 h to day 5 (Fig. 5A). Unlike ES cells, pNC cells demonstrated a restricted potential as soon as 6 h after induction and were unable to differentiate into mesoderm or endoderm cells fates under low inducing conditions, as assessed by TBXT, TBX6, SOX17 and EOMES expression (Fig. 5B, 5C). We further expanded our analysis to include transcriptional changes of mesoderm genes (TBXT, TBX6, GSC, MIXL1) and endoderm genes (SOX17, FOXA2, EOMES, CXCR4) via RT-qPCR. In agreement with our immunostaining results, under mesoderm or endoderm inducing conditions, pNC cells showed a lack of potential to differentiate towards mesoderm or endoderm within 6 h of induction. This can be seen through very low levels of expression of mesodermal or endodermal genes relative to their expression when differentiated from ES cells (Fig. 5D).

These results strongly suggest that soon after the induction of pNC from pluripotent ES cells, their differentiation potential dramatically changes compared to that of ES cells. Our results elaborate on the issue of cranial NC plasticity, as cranial NC specification results in restricted potential of pNC as seen under mesendoderm inducing signals. Taken together, the work presented here suggests that NC lineage, associated with the early cranial NC, is initiated from pluripotent ES cells with distinct molecular profile and a restricted stem cell potential under the inducing signals from the Wnt/β-catenin pathway (Fig. 6).

4. Discussion

In this report, we have characterized molecularly and functionally the formation of hNC cells from pluripotent hES. The model of sequential segregation of stem cell potential is based on the epigenetic proposal from Waddington (Waddington, 1966) suggesting that cell fates are progressively restricted in their differentiation potential compared to their precursors, with the formation of the three embryonic germ layers being a major step towards lineage restriction. The neural crest has been regarded as an enigmatic embryonic stem cell population based on its potential to contribute to many, but not all, derivatives commonly considered to be of ectoderm and mesoderm origin. To address this unique stem cell potential of NC, it has been suggested that the initial specification of cranial NC occurs prior to gastrulation and formation of definitive germ layers, thus maintaining more plasticity within NC cells than the ectodermal and mesodermal cell fates (Basch et al., 2006; Betters et al., 2018; Prasad et al., 2020). However, a distinct molecular character of these early specified NC cells from the pluripotent ES cells has not yet been addressed. Such analyses are further complicated by the heterogenous nature of the early embryo.

Here, we took advantage of our robust and synchronous human NC model to identify the early specification of human cranial NC from ES cells at both molecular and functional levels. Our human NC model is based on activation of the Wnt/β-catenin signaling pathway

in ES cells, which is required for NC formation in multiple embryonic model systems (Basch et al., 2006; Betters et al., 2018; Garcia-Castro et al., 2002; Ikeya et al., 1997; LaBonne and Bronner-Fraser, 1998; Mancilla and Mayor, 1996; Patthey et al., 2008, 2009, n.d.; Saint-Jeannet et al., 1997; Stuhlmiller and García-Castro, 2012a). Wnt/β-catenin signaling has also been documented in earlier regions of the chick epiblast containing pNC cells (Wilson et al., 2001). Data from our human NC model suggests distinct molecular characteristics of ES and pNC states from the earliest times tested, and a dramatic limitation in the capacity of these early NC precursors to acquire mesoderm and endoderm markers. Induction through Activin or FGF – which effectively differentiates ES cells towards endoderm and mesoderm, respectively – are unable to do the same with pNC just 6 h after induction. These cells have clearly initiated a path towards the NC lineage, and lose the plasticity that is a hallmark of ES cells. We note that these experiments do not assess whether pNC are committed to the NC lineage, but shed light on the early specification state of pNC and their restricted potential compared to PSCs. Indeed, the fields of cellular reprogramming and induced pluripotent stem cells capitalizes on the ability of cells to overcome hurdles of committed cell fate. However, our study explores differences in the innate capacity of cells to engage or initiate different cell fates. To assess the difference between the pluripotent stem cell state and the specified state of NC cell with restricted stem cell potential, we utilized the minimal inductive signal that is required for pluripotent stem cells to robustly form mesendoderm. Our novel assay attempts to identify the minimum signaling requirements that induces strong and consistent differentiation of pluripotent stem cells. In turn, this exposes important differences in stem cell potential between ES and pNC cells. Similarly, functional terminal differentiation assays validate that competencies for differentiation are distinct between ES and NC cells during later a developmental stage (day 5 NC). NC generate expected NC-terminal derivatives readily, while ES fail to do so under the same conditions. Certainly, ES cells can generate all these derivatives under other conditions – after acquiring intermediate transient fates such as NC, mesoderm or ectoderm – but under the same circumstances that differentiate hNC, they are unable to generate NC terminal derivatives. While this result is not surprising, it provides further support that hNC cells have a distinct multipotent potential compared to the pluripotent stem cells from which they are derived and are in agreement with grafting experiments of mammalian NC cells in pre-implantation mouse embryos (Jaenish, 1985). A recent report in *Xenopus* embryos equated pluripotent stem cells and NC, and suggested that early NC cells retain expression of some pluripotency genes and pluripotent differentiation capacity (Buitrago-Delgado et al., 2015). However, our human NC study suggests that cranial NC precursors have a restricted stem cell potential, distinct from pluripotent ES cells, as demonstrated by their inability to differentiate into mesendodermal cell fates as early as 6 h post Wnt-based induction. While early pNC cells do express some pluripotency markers, we observe clear changes in stoichiometric levels of multiple pluripotency genes in pNC cells from a PSC state.

Our human NC model further provides a unique glimpse into the early molecular changes of pNC cells. Analysis of core pluripotency gene promoters as well as NC gene promoters for epigenetic changes in the form of active or repressed histone marks revealed a rapid change in epigenetic status of pNC cells from ES cells. Changes in epigenetic status have been associated with cell fate choices (Dileep et al., 2019; Spivakov and Fisher, 2007; Voigt et al.,

2013b). Our work addresses the epigenetic status of pNC cells at an early stage of human cranial NC formation and eludes to the distinct molecular character of pNC. The rapid acquisition (within 6–12hrs) of activation marks (H3K4me3, H3K27ac) and repressive marks (H3K27me3) at the NC genes promoters suggest a transition of these cells into the NC state from the pluripotent stem cell state. Further analysis at the genome-wide scale will be needed to address the accessibility and epigenetic state of all known NC genes. The observed restricted potential and change in epigenetic status of pNC, compared to ES, is also marked by stoichiometric changes in the expression of stem cell genes (OCT4, SOX2, KLF4, NANOG). It is well established that stoichiometry of stem cell factors is crucial in the establishment and maintenance of the pluripotent stem cell state (Papapetrouet al., 2009b; Boer et al., 2007), and that stoichiometric changes result in the loss of pluripotency (Carey et al., 2011; Niwa et al., 2000; Papapetrou et al., 2009b). The maintenance of expression of some of the other stemness genes (Fig. 2A) can be explained based on their context-dependent role in NC development. The stem cell factors LIN28 has been documented to play a role during later stages of NC development as well as NC-related pathologies (Shyh-Chang and Daley, 2013), while the expression of OCT4, KLF4 and NANOG during later stages NC development has also been suggested (Thomas et al., 2008; Lignell et al., 2017; Wang et al., 2012). The changes we observe in ES gene expression in pNC at 6 h, including the downregulation of TFCP2L1 which is responsible for maintenance of expression of core ES genes (Liu et al., 2017; Sun et al., 2018), along with unbalanced stoichiometry of core stemness genes, and the activation of NC-I genes, strongly support a transition in cell fate from ES to pNC rapidly after NC induction. The early NC genes PAX3, PAX7, and ZIC3 are expressed at lower levels compared to the later NPB/NC stages in a homogenous manner. Interestingly, the expression of PAX3/PAX7 increases robustly by day 3 in some cells initially, with uniform expression by day 5. The protein expression of PAX3/7 and ZIC3 at such an early stage in pNC cells of amniotes potentially suggests an even earlier role of these factors in cranial NC specification than previously documented (Basch et al., 2006). Importantly, expression of ectodermal and mesodermal genes was significantly lower in NC precursors when compared to the ectodermal and mesodermal precursors at the same time points. In our previous study we have demonstrated that NC cells in our human NC culture system arise independent of neural ectodermal contributions, as knockdown of Pax6 (early neural determinant) does not affect NC differentiation (Leung et al., 2016). Further functional characterization of the role of other ectodermal factors during NC specification is needed. Thus, at the molecular level, our data indicates a change in stem cell potential soon after Wnt/β-catenin signaling activation, from a pluripotent state towards a more restricted NC cell fate independent of ectodermal gene expression.

Given the essential and well documented role of Wnt/β-catenin signaling during early NC formation in other vertebrate model systems (Garcia-Castro et al., 2002; Ikeya et al., 1997; LaBonne and Bronner-Fraser, 1998; Leung et al., 2016; Saint-Jeannet et al., 1997), we validated the conserved role of Wnt/β-catenin in inducing early pNC genes as well as later NPB and NC genes. The early changes in expression mediated by Wnt/β-catenin signaling are critical, as knockdown of GBX2, a known Wnt/β-catenin target in NC formation, affected the majority of NPB and NC genes tested, in agreement with findings in *Xenopus* (Li et al., 2009). While GBX2 plays a crucial role during NC formation temporally, there are

other likely factors that form a part of β-catenin transcriptional response during early NC specification (first 48 h) that remain to be identified. Our study for the first time identifies an early conserved role of GBX2 during early NC specification in a mammalian model system. Further analysis of transcriptional changes leading to NC specification from ES cells will help in identifying the regulatory network involved during these early steps of NC induction. It is essential to assess this early NC regulatory network, especially in light of new studies exposing a predisposition of blastomeres towards specific cell fates, based on the relative expression ratios of different lineage specifiers (Shi et al., 2015). To understand the cell fate specification of different lineages *in vivo*, positional single cell transcriptional analysis at the blastula stage is needed to identify the network structure of individual cells to ascertain their predisposed cell fates. Based on our experiments in our *in vitro* human NC model, we propose that prospective NC cells with a distinct molecular profile represent the earliest phase in cranial human NC cell development specified from ES cells, in agreement with our recent findings of pNC population in the blastula stage chick epiblast (Prasad et al., 2020).

5. Conclusion

In summary, our study establishes the expression profiles of a comprehensive set of genes involved in NC development at high temporal resolution during 5 days of human NC formation. We further elaborate temporally the transcriptional targets of β-catenin and identify GBX2 as one of the early pNC factors that is required for human NC formation. Furthermore, we provide clear evidence that NC even from early stages (pNC) is functionally distinct from pluripotent stem cells with a restricted stem cell potential. Our data strongly suggest that hNC specification is characterized by stoichiometric changes in expression of pluripotency genes, expression of early pNC genes, and clear functional limitations in the capacity of pNC to form mesendoderm. We propose a human cranial NC model of specification from an ES cell state, where NC cells are endowed with multipotent potential to form mesectodermal derivatives. Our work provides valuable insights into hNC development for future studies to further elaborate on genes involved in early hNC specification.

Supplementary Material

Refer to Web version on PubMed Central for supplementary material.

Acknowledgements

We thank UCR Genomics core, UCR Microscopy and Imaging Core Facility and the UCR Stem Cell Core Facility (California Institute for Regenerative Medicine (CIRM) funded shared facility). We thank Dr. Sika Zhang (UC Riverside) for his generous support in use of the Applied Biosystems QuantStudio 6 Real-Time PCR System for gene expression analysis, and Dr. Nicolas DiPatrizio (UC Riverside) for use of the BioRad ChemiDoc for western blot analysis. We are grateful to Dr. Ken Cho (UC Irvine) and Dr. Ira Blitz (UC Irvine) for helpful conversations, suggestions and critical reading of the manuscript.

Funding

This work was funded by NIH grant R01DE017914 and R21DE028112 to M.I.G-C. and R.M.C is funded under F32DE027862.

References

Bang AG, Papalopulu N, Goulding MD, Kintner C, 1999. Expression of Pax-3 in the lateral neural plate is dependent on a Wnt-mediated signal from posterior nonaxial mesoderm. Dev. Biol 212 (2), 366–380. 10.1006/dbio.1999.9319. [PubMed: 10433827]

Basch ML, Bronner-Fraser M, García-Castro MI, 2006. Specification of the neural crest occurs during gastrulation and requires Pax7. Nature 441 (7090), 218–222. [PubMed: 16688176]

Betters E, Charney RM, Garcia-Castro MI, 2018. Early specification and development of rabbit neural crest cells. Dev. Biol 444, S181–S192. [PubMed: 29932896]

Betters E, Liu Y, Kjaeldgaard A, Sundström E, García-Castro MI, 2010. Analysis of early human neural crest development. Dev. Biol 344 (2), 578–592. [PubMed: 20478300]

Boer B, Kopp J, Mallanna S, Desler M, Chakravarthy H, Wilder PJ, Bernadt C, Rizzino A, 2007. Elevating the levels of Sox2 in embryonal carcinoma cells and embryonic stem cells inhibits the expression of Sox2:Oct-3/4 target genes. Nucleic Acids Res. 35, 1773–1786. doi:10.1093/nar/gkm059. [PubMed: 17324942]

Bolande R, 1974. The neurocristopathiesA unifying concept of disease arising in neural crest maldevelopment. Hum. Pathol 5 (4), 409–429.

Bolande R, 1997. Neurocristopathy: its growth and development in 20 years. Fetal Pediatr. Path 17 (1), 1–25.

Bolande RP, 1996. Neurocristopathy: its growth and development in 20 years. Pediatr. Pathol. Labwatoly Med 17, 1–25.

Buitrago-Delgado E, Nordin K, Rao A, Geary L, LaBonne C, 2015. Shared regulatory programs suggest retention of blastula-stage potential in neural crest cells. Science 348 (6241), 1332–1335. [PubMed: 25931449]

Carey B, Markoulaki S, Hanna J, Faddah D, Buganim Y, Kim J, Ganz K, Steine E, Cassady J, Creyghton M, Welstead GG, Gao Q, Jaenisch R, 2011. Reprogramming factor stoichiometry influences the epigenetic state and biological properties of induced pluripotent stem cells. Cell Stem Cell 9 (6), 588–598. [PubMed: 22136932]

Chambers SM, Mica Y, Lee G, Studer L, Tomishima MJ, 2016. Dual-SMAD inhibition/WNT activation-based methods to induce neural crest and derivatives from human pluripotent stem cells. Methods Mol. Biol 1307, 329–343. 10.1007/7651_2013_59. [PubMed: 24301074]

Chambers SM, Qi Y, Mica Y, Lee G, Zhang X-J, Niu L, Bilsland J, Cao L, Stevens E, Whiting P, Shi S-H, Studer L, 2012. Combined small-molecule inhibition accelerates developmental timing and converts human pluripotent stem cells into nociceptors. Nat. Biotechnol 30 (7), 715–720. [PubMed: 22750882]

D'Amour KA, Agulnick AD, Eliazer S, Kelly OG, Kroon E, Baetge EE, 2005. Efficient differentiation of human embryonic stem cells to definitive endoderm. Nat. Biotechnol 23 (12), 1534–1541. [PubMed: 16258519]

Dileep V, Wilson KA, Marchal C, Lyu X, Zhao PA, Li B, Poulet A, Bartlett DA, Rivera-Mulia JC, Qin ZS, Robins AJ, Schulz TC, Kulik MJ, McCord RP, Dekker J, Dalton S, Corces VG, Gilbert DM, 2019. Rapid irreversible transcriptional reprogramming in human stem cells accompanied by discordance between replication timing and chromatin compartment. Stem Cell Rep. 13 (1), 193–206.

Doddrell RDS, Dun X-P, Moate RM, Jessen KR, Mirsky R, Parkinson DB, 2012. Regulation of Schwann cell differentiation and proliferation by the Pax-3 transcription factor. Glia 60 (9), 1269–1278. [PubMed: 22532290]

Etchevers HC, Amiel J, Lyonnet S, 2006. Molecular bases of human neurocristopathies. Adv. Exp. Med. Biol 589, 213–234. 10.1007/978-0-387-46954-6_14. [PubMed: 17076285]

Evans M, 2011. Discovering pluripotency: 30 years of mouse embryonic stem cells. Nat. Rev. Mol. Cell Biol 12 (10), 680–686. [PubMed: 21941277]

Farlie PG, McKeown SJ, Newgreen DF, 2004. The neural crest: basic biology and clinical relationships in the craniofacial and enteric nervous systems. Birth Defect. Res. C 72 (2), 173–189.

Fukuta M, Nakai Y, Kirino K, Nakagawa M, Sekiguchi K, Nagata S, Matsumoto Y, Yamamoto T, Umeda K, Heike T, Okumura N, Koizumi N, Sato T, Nakahata T, Saito M, Otsuka T, Kinoshita S,

Ueno M, Ikeya M, Toguchida J, 2014. Derivation of mesenchymal stromal cells from pluripotent stem cells through a neural crest lineage using small molecule compounds with defined media. PLoS ONE 9, e112291–25. doi:10.1371/journal.pone.0112291. [PubMed: 25464501]

Funa N, Schachter K, Lerdrup M, Ekberg J, Hess K, Dietrich N, Honoŕe C, Hansen K, Semb H, 2015. β-catenin regulates primitive streak induction through collaborative interactions with SMAD2/SMAD3 and OCT4. Cell Stem Cell 16 (6), 639–652. [PubMed: 25921273]

Gans C, Northcutt RG, 1983. Neural crest and the origin of vertebrates: a new head. Science 220 (4594), 268–273. [PubMed: 17732898]

Garcia-Castro MI, Marcelle C, Bronner-Fraser M, 2002. Ectodermal Wnt function as a neural crest inducer. Science 297, 848–851. [PubMed: 12161657]

Glenn Northcutt R, 2005. The new head hypothesis revisited. J. Exp. Zool 304B (4), 274–297.

Gomez GA, Prasad MS, Sandhu N, Shelar PB, Leung AW, García-Castro MI, 2019a. Human neural crest induction by temporal modulation of WNT activation. Dev. Biol 449 (2), 99–106. [PubMed: 30826399]

Gomez GA, Prasad MS, Wong M, Charney RM, Shelar PB, Sandhu N, Hackland JOS, Hernandez JC, Leung AW, García-Castro MI, 2019b. WNT/ β-catenin modulates the axial identity of embryonic stem cell-derived human neural crest. Development 146 (16), dev175604. 10.1242/dev.175604. [PubMed: 31399472]

Hackland JOS, Frith TJR, Thompson O, Marin Navarro A, Garcia-Castro MI, Unger C, Andrews PW, 2017. Top-down inhibition of BMP signaling enables robust induction of hPSCs into neural crest in fully defined, xeno-free conditions. Stem Cell Rep. 9 (4), 1043–1052.

Hackland JOS, Shelar PB, Sandhu N, Prasad MS, Charney RM, Gomez GA, Frith TJR, García-Castro MI, 2019. FGF modulates the axial identity of trunk hPSC-derived neural crest but not the cranial-trunk decision. Stem Cell Rep. 12 (5), 920–933.

Hall BK, 2018. Germ layers, the neural crest and emergent organization in development and evolution. Genesis 56, e23103–9. [PubMed: 29637683]

Hall BK, 2000. The neural crest as a fourth germ layer and vertebrates as quadroblastic not triploblastic. Evol. Dev 2 (1), 3–5. [PubMed: 11256415]

Huang M, Miller ML, McHenry LK, Zheng T, Zhen Q, Ilkhanizadeh S, Conklin BR, Bronner ME, Weiss WA, 2016. Generating trunk neural crest from human pluripotent stem cells. Sci. Rep 6, 1–9. 10.1038/srep19727. [PubMed: 28442746]

Huang S-M, Mishina YM, Liu S, Cheung A, Stegmeier F, Michaud GA, Charlat O, Wiellette E, Zhang Y, Wiessner S, Hild M, Shi X, Wilson CJ, Mickanin C, Myer V, Fazal A, Tomlinson R, Serluca F, Shao W, Cheng H, Shultz M, Rau C, Schirle M, Schlegl J, Ghidelli S, Fawell S, Lu C, Curtis D, Kirschner MW, Lengauer C, Finan PM, Tallarico JA, Bouwmeester T, Porter JA, Bauer A, Cong F, 2009. Tankyrase inhibition stabilizes axin and antagonizes Wnt signalling. Nature 461 (7264), 614–620. [PubMed: 19759537]

Ikeya M, Lee SMK, Johnson JE, McMahon AP, Takada S, 1997. Wnt signalling required for expansion of neural crest and CNS progenitors. Nature 389 (6654), 966–970. [PubMed: 9353119]

Jaenish R, 1985. Mammalian neural crest cells participate in normal embryonic development on microinjection into post-implantation mouse embryos. Nature 318, 181–183. [PubMed: 4058595]

Ko SO, Chung IH, Xu X, Oka S, Zhao H.u., Cho ES, Deng C, Chai Y, 2007. Smad4 is required to regulate the fate of cranial neural crest cells. Dev. Biol 312 (1), 435–447. [PubMed: 17964566]

LaBonne C, Bronner-Fraser M, 1998. Neural crest induction in Xenopus: evidence for a two-signal model. Development 125, 2403–2414. [PubMed: 9609823]

Le Douarin NM, 1980. The ontogeny of the neural crest in avian embryo chimaeras. Nature 286 (5774), 663–669. [PubMed: 6106161]

Le Douarin N, Kalcheim C (Eds.), 1999. The Neural Crest. Cambridge University Press.

Le Douarin NM, Dupin E, 2018. The “beginnings” of the neural crest. Dev. Biol 444, S3–S13. [PubMed: 30048640]

Lee ER, Murdoch FE, Fritsch MK, 2007a. High histone acetylation and decreased polycomb repressive complex 2 member levels regulate gene specific transcriptional changes during early embryonic stem cell differentiation induced by retinoic acid. Stem Cells 25 (9), 2191–2199. [PubMed: 17525233]

Lee G, Chambers SM, Tomishima MJ, Studer L, 2010. Derivation of neural crest cells from human pluripotent stem cells. Nat. Protoc 5 (4), 688–701. [PubMed: 20360764]

Lee G, Kim H, Elkabetz Y, Al Shamy G, Panagiotakos G, Barberi T, Tabar V, Studer L, 2007b. Isolation and directed differentiation of neural crest stem cells derived from human embryonic stem cells. Nat. Biotechnol 25 (12), 1468–1475. [PubMed: 18037878]

Leung AW, López-Giráldez F, Broton C, Lin K, Prasad MS, Hernandez JC, Xiao AZ, García-Castro MI, 2019. Pre-Border Gene Foxb1 Regulates the Differentiation Timing and Autonomic Neuronal Potential of Human Neural Crest Cells. bioRxiv, 646026. 10.1101/646026.

Leung AW, Murdoch B, Salem AF, Prasad MS, Gomez GA, García-Castro MI, 2016. WNT/β-catenin signaling mediates human neural crest induction via a pre-neural border intermediate. Development 143 (3), 398–410. [PubMed: 26839343]

Li B, Kuriyama S, Moreno M, Mayor R, 2009. The posteriorizing gene Gbx2 is a direct target of Wnt signalling and the earliest factor in neural crest induction. Development 136 (19), 3267–3278. [PubMed: 19736322]

Lignell A, Kerosuo L, Streichan SJ, Cai L, Bronner ME, 2017. Identification of a neural crest stem cell niche by spatial genomic analysis. Nat. Commun 8 (1) 10.1038/s41467-017-01561-w.

Liu K, Zhang Y, Liu D, Ying Q-L, Ye S, 2017. TFCP2L1 represses multiple lineage commitment of mouse embryonic stem cells through MTA1 and LEF1. J. Cell. Sci 130 (22), 3809–3817. [PubMed: 28982712]

Mancilla A, Mayor R, 1996. Neural crest formation in Xenopus laevis: mechanisms of Xslug induction. Dev. Biol 177 (2), 580–589. [PubMed: 8806833]

Menendez L, Yatskievych TA, Antin PB, Dalton S, 2011. Wnt signaling and a Smad pathway blockade direct the differentiation of human pluripotent stem cells to multipotent neural crest cells. Proc. Natl. Acad. Sci 108 (48), 19240–19245. [PubMed: 22084120]

Mica Y, Lee G, Chambers S, Tomishima M, Studer L, 2013. Modeling neural crest induction, melanocyte specification, and disease-related pigmentation defects in hESCs and patient-specific iPSCs. Cell Rep. 3 (4), 1140–1152. [PubMed: 23583175]

Niwa H, Miyazaki J-I, Smith AG, 2000. Quantitative expression of Oct-3/4 defines differentiation, dedifferentiation or self-renewal of ES cells. Nat. Genet 24 (4), 372–376. [PubMed: 10742100]

Oka K, Oka S, Chai Y, 2009. The role of TGF-β signaling in cranial neural crest cells during mandibular and tooth development. J. Oral Biosci 51 (3), 143–150.

O'Rahilly R, Müller F, 2007. The development of the neural crest in the human. J. Anatomy 211 (3), 335–351.

Papapetrou EP, Tomishima MJ, Chambers SM, Mica Y, Reed E, Menon J, Tabar V, Mo Q, Studer L, Sadelain M, 2009b. Stoichiometric and temporal requirements of Oct4, Sox2, Klf4, and c-Myc expression for efficient human iPSC induction and differentiation. Proc. Natl. Acad. Sci 106, 12759–12764. 10.1073/pnas.0904825106. [PubMed: 19549847]

Patthey C, Edlund T, Gunhaga L, 2009. Wnt-regulated temporal control of BMP exposure directs the choice between neural plate border and epidermal fate. Development 136 (1), 73–83. [PubMed: 19060333]

Patthey C, Gunhaga L, Edlund T, 2008. Early Development of the central and peripheral nervous systems is coordinated by Wnt and BMP signals. PLoS ONE 3, e1625–10. doi:10.1371/journal.pone.0001625. [PubMed: 18286182]

Pera MF, Trounson AO, 2004. Human embryonic stem cells: prospects for development. Development 131, 5515–5525. 10.1242/dev.01451. [PubMed: 15509763]

Petruk S, Cai J, Sussman R, Sun G, Kovermann SK, Mariani SA, Calabretta B, McMahon SB, Brock HW, Iacovitti L, Mazo A, 2017. Delayed accumulation of H3K27me3 on nascent DNA is essential for recruitment of transcription factors at early stages of stem cell differentiation. Mol. Cell 66 (2), 247–257.e5. [PubMed: 28410996]

Prasad MS, Charney RM, García-Castro MI, 2019. Specification and formation of the neural crest: perspectives on lineage segregation. Genesis 57 (1), e23276. 10.1002/dvg.v57.110.1002/dvg.23276. [PubMed: 30576078]

Prasad MS, Sauka-Spengler T, LaBonne C, 2012. Induction of the neural crest state: control of stem cell attributes by gene regulatory, post-transcriptional and epigenetic interactions. Dev. Biol 366 (1), 10–21. [PubMed: 22583479]

Prasad MS, Uribe-Querol E, Marquez J, Vadasz S, Yardley N, Shelar PB, Charney RM, García-Castro MI, 2020. Blastula stage specification of avian neural crest. Dev. Biol 458 (1), 64–74. [PubMed: 31610145]

Rada-Iglesias A, Bajpai R, Prescott S, Brugmann SA, Swigut T, Wysocka J, 2012. Epigenomic annotation of enhancers predicts transcriptional regulators of human neural crest. Cell Stem Cell 11 (5), 633–648. [PubMed: 22981823]

Rada-Iglesias A, Bajpai R, Swigut T, Brugmann SA, Flynn RA, Wysocka J, 2011. A unique chromatin signature uncovers early developmental enhancers in humans. Nature 470 (7333), 279–283. [PubMed: 21160473]

Rodda SJ, Kavanagh SJ, Rathjen JR, Rathjen PD, 2002. Embryonic stem cell differentiation and the analysis of mammalian development. Int. J. Dev. Biol. Saint-Jeannet, J.-P., He, X., Varmus, H.E., Dawid, I.B., 1997. Regulation of dorsal fate in the neuraxis by Wnt-1 and Wnt-3a. Proc. Natl. Acad. Sci 94 (25), 13713–13718.

Sasai Y, 2013. Next-generation regenerative medicine: organogenesis from stem cells in 3D culture. Cell Stem Cell 12 (5), 520–530. [PubMed: 23642363]

Sauka-Spengler T, Bronner-Fraser M, 2008. A gene regulatory network orchestrates neural crest formation. Nat. Rev. Mol. Cell Biol 9 (7), 557–568. [PubMed: 18523435]

Shi J, Chen Q.i., Li X, Zheng X, Zhang Y, Qiao J, Tang F, Tao Y.i., Zhou Q.i., Duan E, 2015. Dynamic transcriptional symmetry-breaking in pre-implantation mammalian embryo development revealed by single-cell RNA-seq. Development 142 (20), 3468–3477. [PubMed: 26395495]

Shyh-Chang N.g., Daley G, 2013. Lin28: Primal regulator of growth and metabolism in stem cells. Cell Stem Cell 12 (4), 395–406. [PubMed: 23561442]

Simoes-Costa M, Bronner ME, 2015. Establishing neural crest identity: a gene regulatory recipe. Development 142 (2), 242–257. [PubMed: 25564621]

Spagnoli FM, Hemmati-Brivanlou A, 2006. Guiding embryonic stem cells towards differentiation: lessons from molecular embryology. Curr. Opin. Genet. Dev 16 (5), 469–475. [PubMed: 16919445]

Spivakov M, Fisher AG, 2007. Epigenetic signatures of stem-cell identity. Nat. Rev. Genet 8 (4), 263–271. [PubMed: 17363975]

Stuhlmiller TJ, García-Castro MI, 2012a. FGF/MAPK signaling is required in the gastrula epiblast for avian neural crest induction. Development 139 (2), 289–300. [PubMed: 22129830]

Stuhlmiller TJ, García-Castro MI, 2012b. Current perspectives of the signaling pathways directing neural crest induction. Cell. Mol. Life Sci 69 (22), 3715–3737. [PubMed: 22547091]

Sun H, You Y.u., Guo M, Wang X, Zhang Y, Ye S, 2018. Tfcp2l1 safeguards the maintenance of human embryonic stem cell self-renewal. J. Cell Physiol 233 (9), 6944–6951. [PubMed: 29323720]

Thomas S, Thomas M, molecular PWH, 2008. Human neural crest cells display molecular and phenotypic hallmarks of stem cells. academic.oup.com doi:10.1093/hmg/ddn235.

Tsankov AM, Gu H, Akopian V, Ziller MJ, Donaghey J, Amit I, Gnirke A, Meissner A, 2015. Transcription factor binding dynamics during human ES cell differentiation. Nature 518 (7539), 344–349. [PubMed: 25693565]

Umeda K, Oda H, Yan Q, Matthias N, Zhao J, Davis B, Nakayama N, 2015. Long-term expandable SOX9+ chondrogenic ectomesenchymal cells from human pluripotent stem cells. Stem Cell Rep. 4 (4), 712–726.

Voigt P, Tee WW, Reinberg D, 2013b. A double take on bivalent promoters. Genes Dev. 27, 1318–1338. 10.1101/gad.219626.113. [PubMed: 23788621]

Waddington CH, 1966. Principles of Development and Differentiation. Macmillan, New York.

Wang Z, Oron E, Nelson B, Razis S, Ivanova N, 2012. Distinct lineage specification roles for NANOG, OCT4, and SOX2 in human embryonic stem cells. Cell Stem Cell 10 (4), 440–454. [PubMed: 22482508]

Wilderman A, VanOudenhove J, Kron J, Noonan JP, Cotney J, 2018. High-resolution epigenomic atlas of human embryonic craniofacial development. Cell Rep. 23, 1581–1597. [PubMed: 29719267]

Wilson S, Rydström A, Trimborn T, Willert K, Nusse R, Jessell TM, Edlund T, 2001. The status of Wnt signalling regulates neural and epidermal fates in the chick embryo. Nature 411 (6835), 325–330. [PubMed: 11357137]

Ying L, Mills J, French D, Gadue P, 2015. OCT4 coordinates with WNT signaling to pre-pattern chromatin at the SOX17 locus during human ES cell differentiation into definitive endoderm. Stem Cell Rep. 5 (4), 490–498.

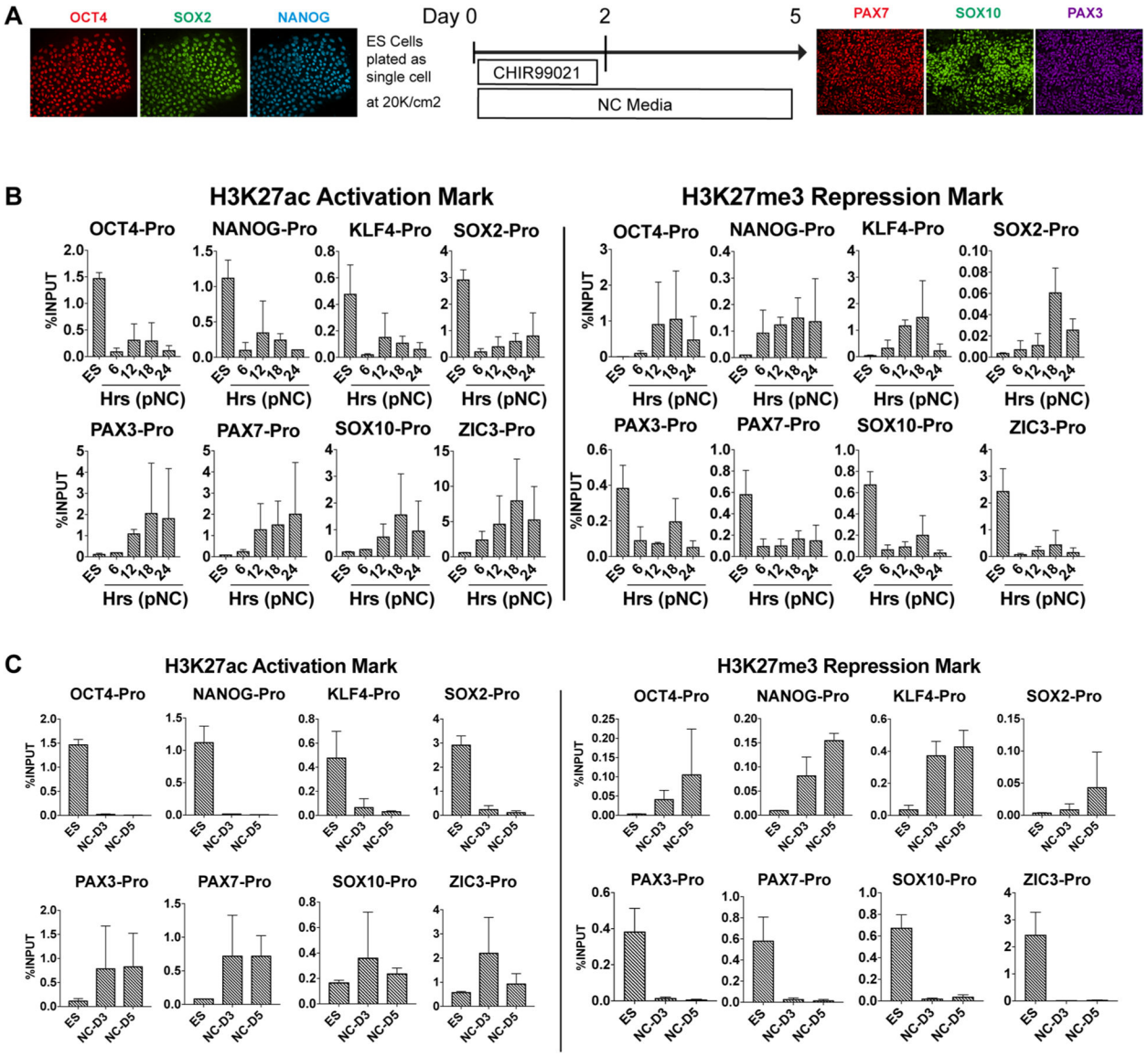

Fig. 1.

Distinct epigenetic state defines a prospective human NC cell state. (A) Schematic of hNC induction model from hES cells using 2 days of Wnt-activation by CHIR treatment. Immunofluorescence of OCT4/SOX2/NANOG on hES cells and PAX3/7/SOX10 on day 5 hNC cells. (B) ChIP-qPCR analysis of core stemness genes (OCT4, NANOG, KLF4) and NC genes (PAX3, PAX7, ZIC3) analyzed at the proximal promoter regions for enrichment of activation (H3K27ac, H3K4me3) and repression (H3K27me3) marks over a time course of every 6 h from ES to pNC for the first 24 h. (C) ChIP-qPCR analysis of core stemness genes (OCT4, NANOG, KLF4) and NC genes (PAX3, PAX7, SOX10, ZIC3) analyzed at the proximal promoter regions for enrichment of activation (H3K27ac, H3K4me3) and repression (H3K27me3) marks at day 3 and day 5 of NC formation and compared to ES cell state. Data is represented as percent input values from 3 independent experimental replicates. Error represent standard error of mean.

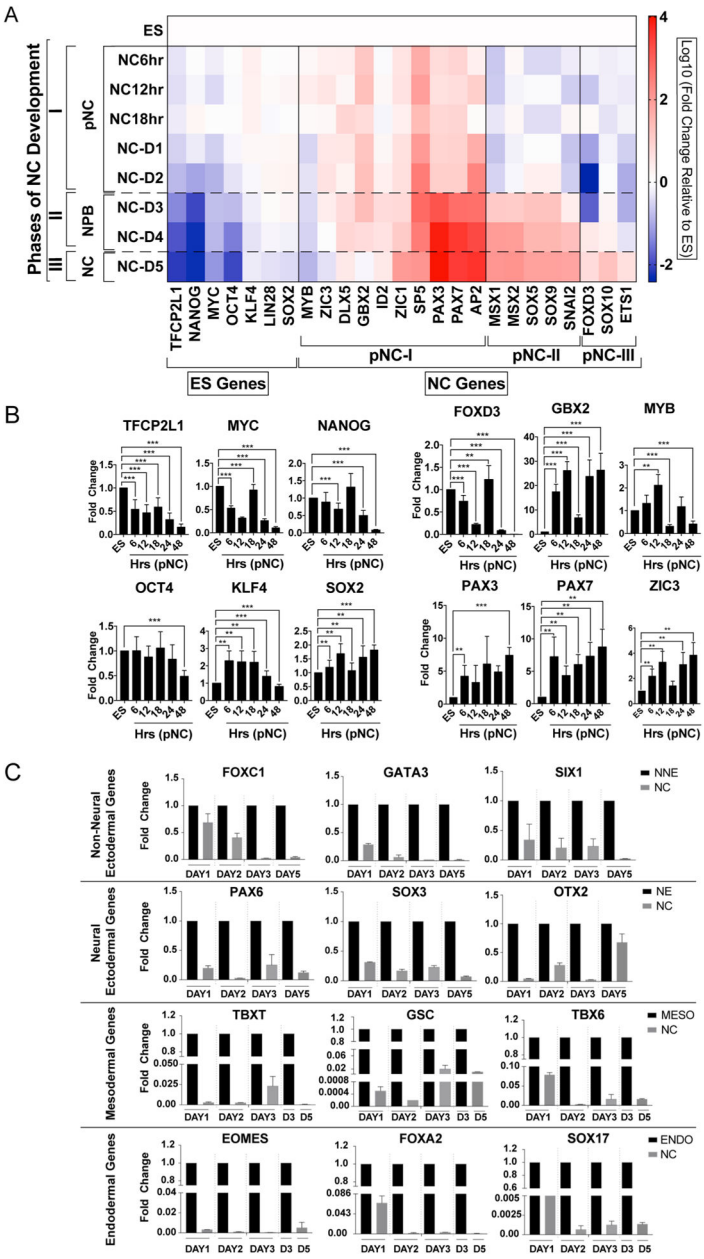

Fig. 2.

Gene expression analysis reveal clear molecular changes in prospective human NC cell state from hES cell state. (A) Gene expression analysis of ES genes and NC related genes over the time course of NC induction from hES cells represented in heat map as log10 fold-change in expression relative to the ES cell state. Heat map is derived from average gene expression from 3 independent biological replicates. Different phases of NC development are highlighted on left side of the heat map. The genes are clustered based on their early to late expression during the 5 days of NC induction. (B) Gene expression analysis over the first 48 h of NC induction of key ES and NC genes with significant changes in expression relative to ES cell state. (C) Gene expression analysis of non-neural ectodermal (NNE), neuroectodermal (NE), mesodermal (Meso) and endodermal (Endo) genes at day 1 to day 5

of NC differentiation from ES cells. Data is represented as fold changes in expression normalized to the presented cell state (NNE/NE/Meso/Endo) at specified time points (day1–5) for the respective genes. Error bars represent SEM from 3 biological replicates. Asterisks indicate statistical significance: *P ≤ 0.05, **P ≤ 0.01, ***P ≤ 0.001, ****P ≤ 0.0001.

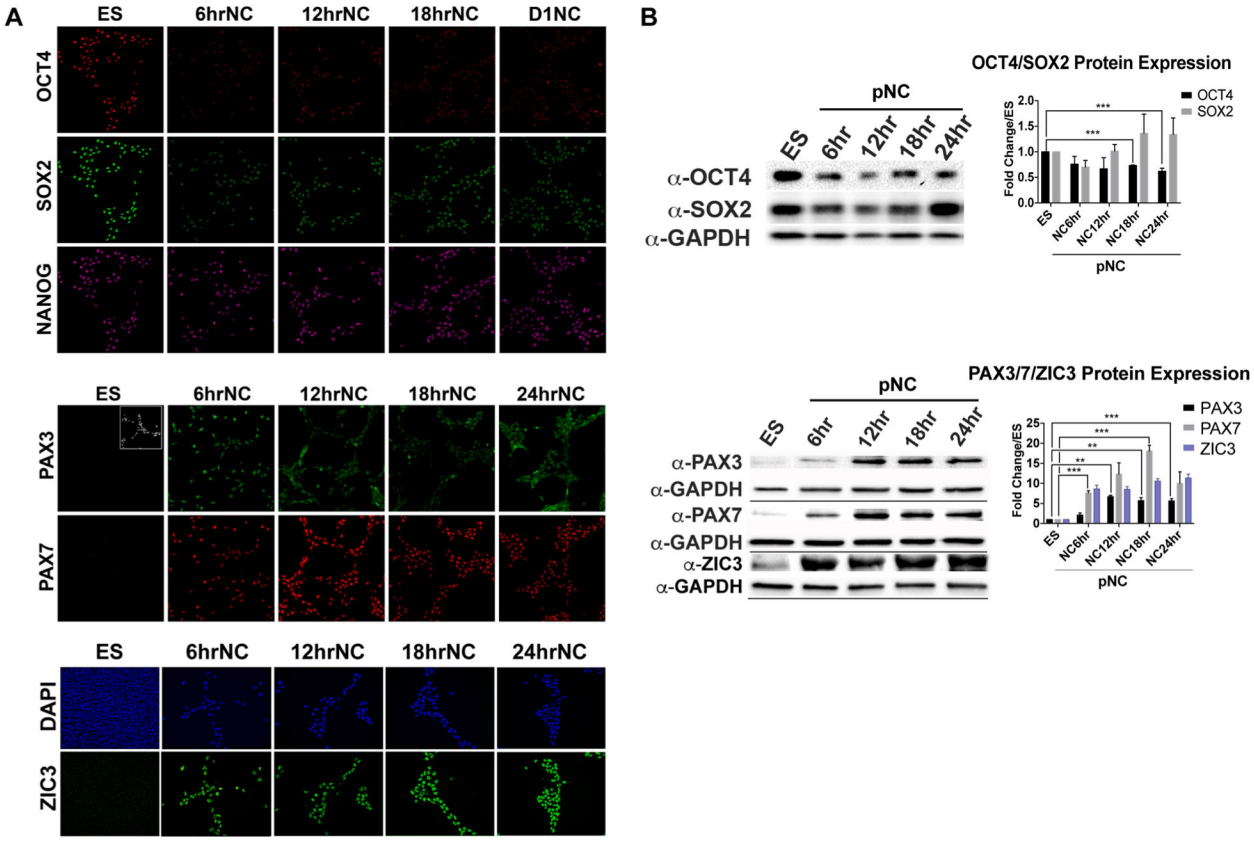

Fig. 3.

Stochiometric changes in protein expression of pluripotency genes combined with expression of NC genes characterizes the prospective NC cell state. (A) Immunofluorescence analysis of OCT4, SOX2, NANOG, PAX3, PAX7 and ZIC3 over the first 24 h of NC induction. On the PAX3, PAX7 panel under ES condition, DAPI stained cells are shown in the inset. (B) Immunoblot analysis of protein levels of ES genes (OCT4/SOX2) and NC genes (PAX3/PAX7/ZIC3) over the first 24 h of NC induction represented with quantification of fold change in pixel density relative to GAPDH and normalized to ES cells from three independent biological replicates. Error bars represent SEM from 3 biological replicates. Asterisks indicate statistical significance: * **P ≤ 0.01, ***P ≤ 0.001.

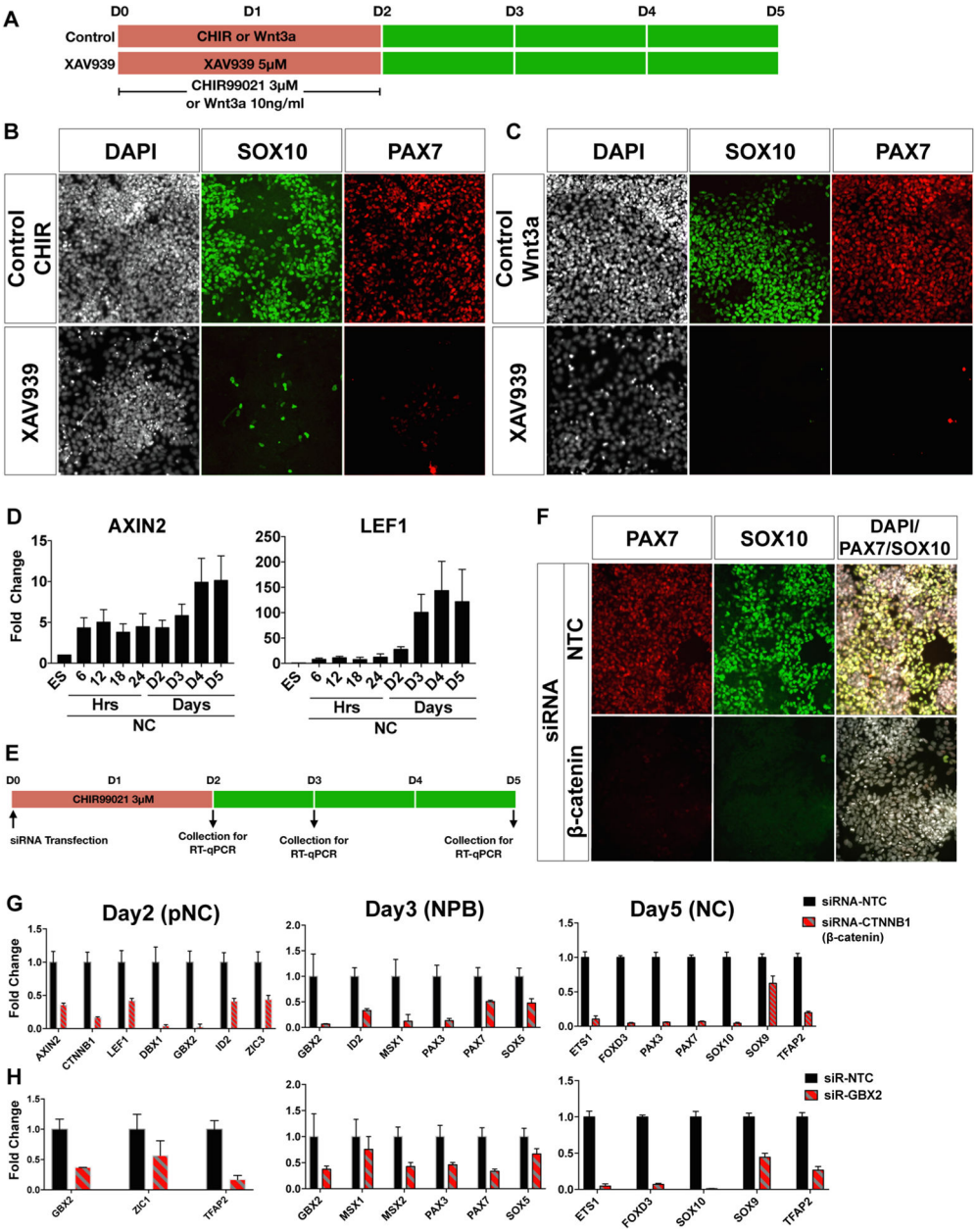

Fig. 4.

Wnt/β-catenin signaling is essential for human NC formation. (A) Schematic depicting NC induction protocol and XAV939 mediated inhibition of Wnt/ β-catenin signaling induced either via CHIR99021 or Wnt3a mediated treatment of hES cells for 2 days. (B) Immunofluorescence of day 5 NC cells treated with CHIR and XAV939 show loss of SOX10/PAX7 expression compared to the control CHIR only condition. (C) Day 5 NC cells treated with Wnt3a and XAV939 show loss of SOX10/PAX7 expression compared to the control Wnt3a only condition. (D) RT-qPCR expression analysis of AXIN2 and LEF1 from 6 h pNC to day 5 NC cell state. Fold change in expression is represented as relative to ES cell state. (E) Schematic of siRNA mediated knockdown in NC induction protocol with collection time points highlighted. (F) Immunofluorescence of day 5 NC cells treated with

CTNNB1 (β-catenin) siRNA and non-targeting control (NTC) siRNA shows complete loss of SOX10/PAX7 expression. (G) Temporal RT-qPCR analysis of day 2, day 3 and day 5 NC genes upon CTNNB1 (β-catenin) siRNA mediated knockdown. Data is represented as relative expression normalized to non-targeting control (NTC) siRNA. (H) Temporal RT-qPCR analysis of day 2, day 3 and day 5 NC genes upon GBX2 siRNA mediated knockdown and normalized to non-targeting control (NTC) siRNA. All experiments were done in experimental replicates of 3, with error bars representing the standard error of mean.

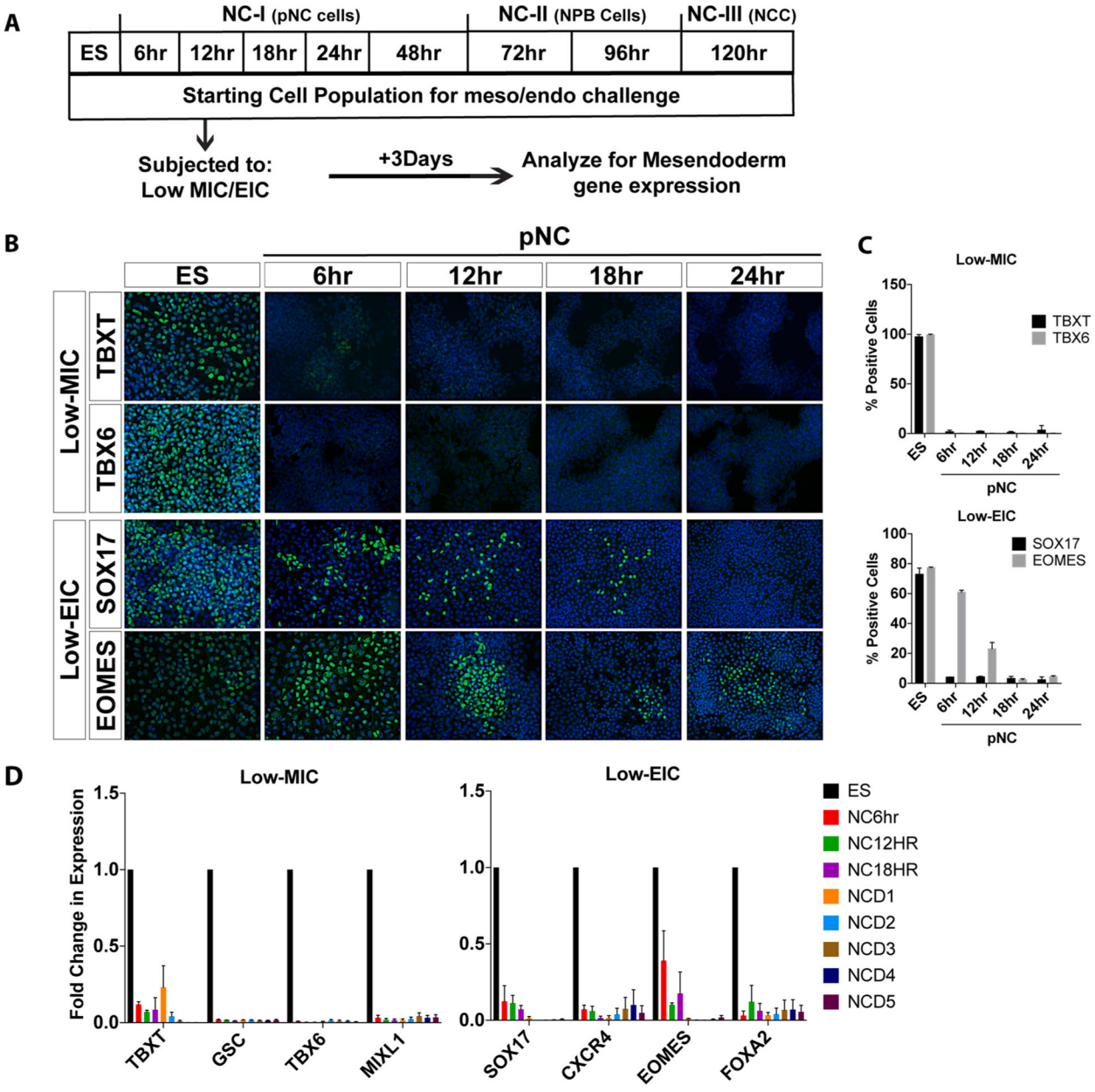

Fig. 5.

Prospective NC cells exhibit a restricted potential to differentiate towards mesendoderm fate. (A) Schematic representation of specification assay analyzing the potential of ES and different states of NC cells to differentiate towards the mesendoderm lineages. (B) Immunofluorescence analysis of mesodermal (TBXT, TBX6) and endodermal (SOX17, EOMES) markers after challenging ES cells and pNC cells within the first 24 h to differentiate into mesendodermal cell fates under low mesoderm/endoderm inducing conditions (MIC/EIC). (C) Quantification of cells represented as percent positive for TBXT, TBX6, SOX17, and EOMES after differentiation of ES cells and pNC during first 24 h of NC induction towards mesendodermal cell fate. (D) Gene expression analysis of mesodermal and endodermal genes after differentiation of ES cells and pNC during the full-

time course of NC induction (5 days) towards mesendodermal cell fate. Gene expression is represented as fold change in expression relative to gene expression in cells differentiated from ES cells. Error bars represent SEM from 3 biological replicates.

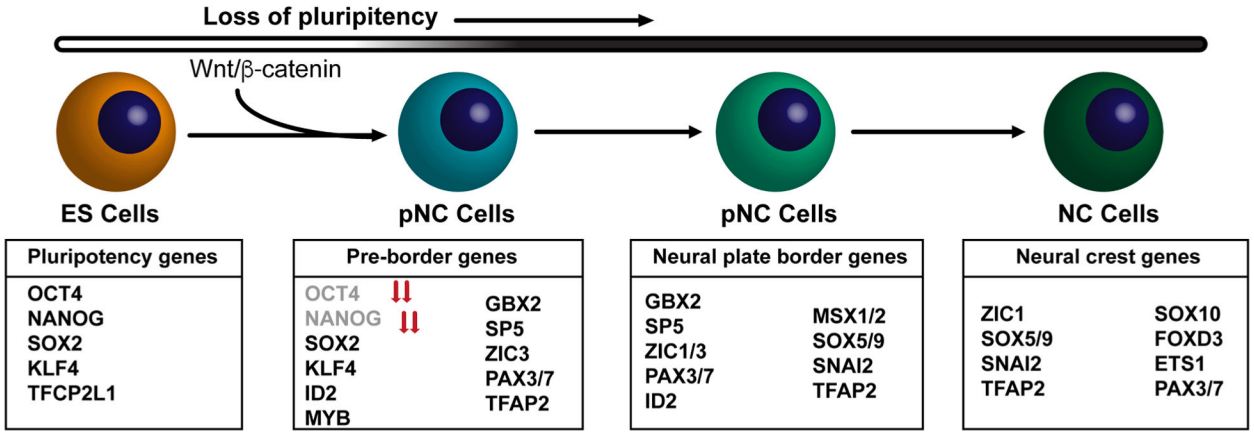

Fig. 6.

Model of NC cell fate specification from embryonic stem cells. Based on our study, the model suggests specification of prospective NC (pNC) from embryonic stem cells induced by Wnt/β-catenin signaling and characterized by loss of pluripotency. Based on the expression of cluster of genes known to be expressed in embryonic stem cells, neural plate border and neural crest cells, we have established three phases of human neural crest specification. The earliest phase, pre-Border (pB), is composed of a unique set of genes including direct Wnt/β-catenin targets as well as some of the known neural crest genes. This phase was also identified by low levels of OCT4/NANOG expression. Neural plate border (NPB) and neural crest (NC) phases follow the pre-Border phase with expression of characteristic NPB and NC markers also documented in model organisms.